Mutagenic analysis of Hazara nairovirus non-translated regions during single and multi-step growth identifies both attenuating and functionally-critical sequences for virus replication

Daniele F. Mega[1], Jack Fuller[1], Beatriz Álvarez-Rodríguez[1], Jamel Mankouri[1], Roger Hewson[2], John N. Barr[1$]

[1]School of Molecular and Cellular Biology, University of Leeds, Leeds, LS2 9JT, United Kingdom

[2]National Infection Service, Public Health England, Porton Down, Salisbury SP4 0JG, United Kingdom

Running Title: Mutational analysis of HAZV non-translated regions

Keywords: Hazara virus, reverse genetics, attenuation, mutagenesis.

Word Count: Abstract 249; Importance 147; Main text (excluding references) - 5423

[$]To whom correspondence should be addressed Tel: 44-113-3438069; E-mail: j.n.barr@leeds.ac.uk

ABSTRACT

Hazara nairovirus (HAZV) is a member of the *Nairoviridae* family within the *Bunyavirales* order, and closely-related to Crimean-Congo hemorrhagic fever virus that is responsible for severe and fatal human disease. The HAZV genome comprises three segments of negative sense RNA named S, M and L, with non-translated regions (NTRs) flanking a single open reading frame. NTR sequences regulate RNA synthesis, and by analogy with other segmented negative sense RNA viruses, may direct activities such as virus assembly and innate immune modulation. The terminal-proximal nucleotides of 3' and 5' NTRs exhibit extensive terminal complementarity; the first eleven nucleotides are strictly conserved and form promoter element (PE) 1, with adjacent segment-specific nucleotides forming PE2. To explore the functionality of NTR nucleotides within the context of the nairovirus multiplication cycle, we designed infectious HAZV mutants bearing successive deletions throughout both S segment NTRs. Fitness of rescued viruses was assessed in single-step and multi-step growth, which revealed the 3' NTR was highly tolerant to change whereas several deletions of centrally-located nucleotides within the 5' NTR led to significantly reduced growth, indicative of functional disruption. Deletions that encroached upon PE1 and PE2 ablated virus growth, and identified additional adjacent nucleotides critical for viability. Mutational analysis of PE2 suggest its signalling ability relies solely on inter-terminal base pairing, and is an independent *cis*-acting signalling module. This study represents the first mutagenic analysis of nairoviral NTRs in the context of the infectious cycle, and the mechanistic implications of our findings for nairovirus RNA synthesis are discussed.

IMPORTANCE

Nairoviruses are a group of RNA viruses that include many serious pathogens of humans and animals, including one of the most serious human pathogens in existence, Crimean-Congo hemorrhagic fever virus. The ability of nairoviruses to multiply and cause disease is controlled in major part by nucleotides that flank the 3' and 5' ends of nairoviral genes, called non-translated regions (NTRs). NTR nucleotides interact with other virus components to perform critical steps of the virus multiplication cycle such as mRNA transcription and RNA replication, with other roles likely. To better understand how NTRs work, we performed the first comprehensive investigation of the importance of NTR nucleotides in the context of the entire nairovirus replication cycle. We identified both dispensable and critical NTR nucleotides, as well as highlighting the importance of 3' and 5' NTR interactions in virus growth, thus providing the first functional map of the nairovirus NTRs.

INTRODUCTION

The *Bunyavirales* order encompasses a diverse collection of over 500 segmented, enveloped RNA viruses that infect a broad range of hosts including humans, animals, insects and plants. The *Nairoviridae* family is one of 12 families within this order, which currently includes 12 distinct species (1). Nairoviruses are tick-borne, being specifically-associated with hard ticks of the *Ixodid* family, with transmission to mammalian and avian hosts occurring through acquisition of a blood meal. Nairoviruses are the causative agents of serious or fatal disease in animals, with humans representing dead-end hosts. The family is named after Nairobi sheep disease virus (NSDV), which causes disease in susceptible goats and sheep that carries a case-fatality rate of around 80% and results in considerable economic impact

(2). Crimean-Congo hemorrhagic fever virus (CCHFV) is a nairovirus of great clinical importance, responsible for a devastating disease in humans known as Crimean-Congo hemorrhagic fever (CCHF), which exhibits a case-fatality rate of around 30%, rising to 80% in specific outbreaks (3). Concerns are growing over the spread and emergence of CCHFV due to the changing habitat of the tick vector in response to climate change, a threat validated by the recent cases of CCHF in northern Spain (4). Due to the severe outcome of CCHFV infection, paired with the lack of options for treatment or prevention of CCHF, this virus is one of a select group of human pathogens classified in Hazard Group 4 by the Advisory Committee on Dangerous Pathogens. In contrast, Hazara nairovirus (HAZV) is not associated with human disease, despite being closely related to CCHFV, sharing the same CCHFV serogroup within the *Nairoviridae* family, as well as structural and functional properties (5–7). In view of the lack of HAZV-associated human disease, it can be handled under relatively unrestrictive biosafety level 2 (BSL-2) containment protocols. HAZV represents a valuable model system with which to gain knowledge of the nairovirus multiplication cycle.

All nairoviruses possess a tri-segmented negative stranded RNA genome and share a common genetic organisation: The three genomic segments are named small (S), medium (M) and large (L) based on their relative sizes, and each acts as the template for transcription of a single mRNA. The S segment mRNA encodes the major nucleocapsid protein (N), the M segment mRNA encodes a glycosylated polyprotein precursor (GPC) that is cleaved into envelope spike proteins Gn and Gc, and the L segment mRNA encodes the RNA-dependant RNA polymerase (RdRp) responsible for transcription and replication of the three RNA segments. An additional open reading frame (ORF) within the CCHFV S segment, accessed by ambisense

100 transcription of its antigenome, has been reported to express a non-structural protein
101 NSs with a role in modulating apoptosis (8), and the cleavage of Gn and Gc moieties
102 from the M segment-specific polyprotein is predicted to yield a polypeptide that may
103 represent the non-structural NSm.

104 By analogy with other bunyaviruses, the RNA synthesis activities of the three
105 nairovirus RNA segments is predicted to be controlled by nucleotide sequences within
106 3' and 5' non-translated regions (NTRs), which flank the S, M and L ORFs. Of all the
107 members of the *Bunyavirales* order, perhaps the best studied in terms of the
108 mechanism of RNA synthesis are Bunyamwera virus (BUNV) and LaCrosse virus
109 (LACV) of the *Peribunyaviridae* family, for which a combination of functional (9–18)
110 and structural studies (19) have elucidated roles for individual nucleotides from within
111 their respective NTRs. The terminal nucleotides of 3' and 5' NTRs exhibit terminal
112 complementarily and such sequences have been shown to bind to, and influence the
113 activity of, the viral RdRp (19), promoting primer-dependant transcription to yield a 5'
114 capped mRNA, as well as to perform primer-independent replication that results in the
115 synthesis of a full-length copy of the genome template.

116 The first eleven nucleotides located at the extreme termini of all three LACV
117 segments are strictly conserved and have been shown to form independent RNA
118 secondary structures that interact with the RdRp at separate sites (19). For BUNV,
119 segment-specific nucleotides at subsequent positions 12-15 are required to form
120 canonical Watson-Crick base-pairing with corresponding nucleotides at the opposite
121 end of the template (10, 20, 21), and together, these RdRp-RNA and RNA-RNA
122 interactions are proposed to account for the pseudo-circular appearance of BUNV and
123 LACV RNPs (22, 23). While sequence changes within the eleven strictly-conserved
124 terminal proximal nucleotides has profound influence on promoter function, the identity

of adjacent nucleotides 12-15 is highly tolerant of nucleotide change providing their inter-terminal Watson-Crick base-pairing potential is maintained. Just 17 terminal proximal nucleotides from 3' and 5' NTRs are required to build up the minimal BUNV transcription and replication promoters (24), and with the exception of a transcription termination signal within the BUNV genomic 5' NTR (12), roles of the remaining nucleotides within both NTRs is currently unclear. NTR deletion analysis in the context of infectious virus has identified functionally important sequences within the BUNV NTRs, with deletion of some regions leading to growth attenuation or lack of virus viability (13, 16) although their specific roles are currently unknown.

For the nairoviruses, little is known of the roles of the 3' and 5' terminal NTRs in either signalling RNA synthesis, or in the broader context of the virus multiplication cycle. As with other bunyavirales members, the NTRs of all nairoviruses comprise highly conserved terminal proximal nucleotides shared by all segments, followed by less conserved regions that are segment specific and extend for between 37-82 nucleotides at the genomic 3' end and 137-242 nucleotides at the genomic 5' end (Fig 1A). The variation in length between the 3' and 5' NTRs across all three segments is striking and raises the possibility that the longer NTRs may contain redundant sequences, or alternatively, may contain signals that confer additional segment-specific properties within the context of the virus replication cycle.

A first and recent study to define nairovirus NTR functionality employed HAZV mini-genomes to describe promoter elements (PEs) that were involved in the signalling of reporter activity as a marker for RNA synthesis (25); PE1 comprised strictly conserved 3' and 5' terminal-proximal sequences, whereas PE2 comprised a GC-rich sequence that was predicted to form inter-terminal Watson-Crick pairings, similar to that described previously for BUNV (10, 20). PE1 and PE2 were found to be

150 separated by a ‘spacer’ region, which exhibited a critical requirement for short length
151 and lack of base-pairing ability (Fig 1B).

152 We recently reported the establishment of a reverse genetics system for HAZV
153 with the capability to efficiently generate infectious HAZV from recombinant sources
154 (26). This system represents a valuable tool with which to better understand the HAZV
155 multiplication cycle, and by extrapolation, that of other nairoviruses including those
156 requiring high containment facilities for their study. Here, we describe the first
157 mutagenic analysis of the 3’ and 5’ NTRs of the HAZV S segment in the context of
158 infectious virus. Our intention was to identify both dispensable and also critical
159 sequences within the NTRs in order to better understand their roles in promoting HAZV
160 multiplication throughout the entire infectious cycle. A total of 26 recombinant HAZV
161 variants in which successive blocks of 3’ and 5’ S segment NTR sequences were
162 deleted, and analysis of growth of the resulting rescued viruses identified several
163 sequences that impacted virus growth and infectivity, and confirmed the requirement
164 of potential inter-terminal base pairing within PE2 for efficient gene expression.
165

166 **RESULTS**
167

168 **Mutagenesis strategy to identify NTR sequences critical for virus viability.** To
169 assess the roles of both 3’ and 5’ NTRs in the HAZV multiplication cycle, we exploited
170 our recently reported three-plasmid system for the rescue of infectious HAZV (strain
171 JC280), in which expression of S, M and L anti-genomic RNAs was driven by
172 bacteriophage T7 RNA polymerase (T7RNAP) in hamster-origin BSRT7 cells (26).
173 Transfection of these plasmids into cells allowed transcription and translation of S, M
174 and L anti-genomes followed by assembly of HAZV RNPs and subsequent generation

of infectious HAZV. An additional plasmid to express exogenous T7RNAP was also included, which increased rescue efficiency.

Our strategy for this study was to generate mutant infectious viruses bearing successive deletions of ten nucleotides throughout both S segment 3' and 5' NTRs, defined here as comprising 3' nucleotides upstream and excluding the start codon, and 5' nucleotides downstream and excluding the stop codon, and to examine their growth and infectivity in BSRT7 and human origin SW13 cells. We chose to perform this analysis using the HAZV S segment due to the small size of its corresponding NTRs, and consequent ease of mutagenesis. A consistent deletion size of ten nucleotides was chosen to allow both NTRs to be covered by a manageable number of mutant viruses, and to provide a sufficiently large deletion window that would increase the likelihood of ablating any critical signals.

A total of seven 3' NTR deletions and thirteen 5' NTR deletions were individually engineered into the corresponding S segment plasmid (Fig 1C), with the changes spanning the entire 3' and 5' NTRs and including previously described PE1 and PE2 (25). Plasmids were named 3'D1 to 3'D7 and 5'D1 to 5'D13, accordingly (Fig 1C), and the full 3' and 5' NTR sequence of all corresponding mutants is shown in Figure S1A and S1B, respectively.

Examining the role of 3' NTR sequences in HAZV multiplication. The panel of seven altered plasmids expressing 3' S segment NTR deletions 3'D1 to 3'D7 were individually transfected into BSRT7 cells along with wild-type (WT) HAZV M and L expressing plasmids to attempt virus rescue. Successful rescue was determined by observing an increase in HAZV N protein abundance in 5-day post transfection (dpt) cell lysates compared to control transfections in which the L segment expression

plasmid was omitted, measured by western blot analysis (Fig 2A). For all attempted virus rescue experiments, 5 dpt supernatants were collected and titres of all rescued viruses calculated by plaque assay on human origin SW13 cells (Fig 2B and C). This analysis provided a measure of virus fitness with supernatant titres consistently correlating with subsequent measure of virus growth. For the most severely attenuated viruses, plaque assay analysis of rescue supernatants also provided a confirmation of viability and allowed examination of plaque size and morphology as an alternative means to assess virus growth properties.

All mutants HAZV 3'D1 to 3'D7 were rescued on the first attempt, and with the exception of 3'D7, genotypes were confirmed by sequence analysis of RT-PCR products spanning the intended sequence changes. Plaque assay analysis revealed mutants 3'D1 to 3'D5 rescued and subsequently multiplied to similar post-transfection supernatant titres as WT HAZV, which was rescued concurrently (Fig 2B and C). Measurement of plaque size as an additional assessment of virus growth characteristics revealed no significant variation, and plaque morphology was consistent displaying the characteristic dark centre, previously referred to as a 'bulls-eye' plaque (27). In contrast, for mutants 3'D6 and 3'D7, SW13 cell plaque assay of 5 dpt supernatants revealed titres of around 10 viruses per ml, suggesting that while these viruses were viable, they were extremely unfit (Fig 2B and C). Repeated transfections confirmed these observations, with equivalent titres obtained on subsequent occasions.

Measurement of the growth characteristics of mutant viruses was achieved by infecting SW13 cell cultures at an MOI of 0.01, and assessing N protein production as a surrogate marker for HAZV gene expression by western blotting at both 18 and 48 hpi time points (Fig 2D and E). N abundance at 18 hpi represented N production in a

single step of virus multiplication within initially-infected cells, whereas the 48 hpi time point also measured the ability of the mutant viruses to assemble and re-infect further cells within the culture. N protein abundance was quantified by densitometry from three independent infections for each mutant used (Fig 2F and G). The titres of mutants 3'D6 and 3'D7 was too low to permit infection at an MOI of 0.01, and even in infections using undiluted titred supernatants (MOI approximately 2 $x10^{-5}$) N protein was not reliably detected at the 18 hpi time point of single-step growth. Comparison between N protein production of mutants 3'D1 to 3'D5 and WT revealed deletion of any of the associated nucleotides has no major impact on virus growth, with no significant differences in N protein abundance at either 18 or 48 hpi time points, with the exception of 3'D3, for which a minor significance difference was recorded.

Examination of the resulting nucleotide sequence of low-viability mutant 3'D6 revealed the changes did not impinge on either PE1 or PE2 (Fig 2H; top schematic), thus revealing a critical role in HAZV viability for residues outside of the established PE1 and PE2 regions. For mutant 3'D7, in which the entire PE2 was deleted (Fig 2H, bottom schematic), its barely detectable multiplication also indicates the PE2 region is required for efficient HAZV multiplication, corroborating and extending previous work by others (25) that concluded the analogous M segment PE2 was required for mini-genome reporter expression.

Examining the role of 5' NTR sequences in HAZV multiplication. The strategy used to attempt rescue of the thirteen 5'NTR mutants was identical to that used for 3'NTR mutants, described above. Recombinant mutant viruses 5'D1 to 5'D11 were rescued on the first attempt, and observation of resulting plaques (Fig 3A) revealed no detectable differences in plaque size or morphology compared to WT. Titres of

250 rescued viruses within post-transfection supernatants were determined (Fig 3B) and
251 all fell within one log of WT HAZV, rescued concurrently. In contrast, viruses 5'D12
252 and 5'D13 failed to rescue on the first attempt, and following further failed attempts,
253 rescue was deemed unattainable.

254 Measurement of the growth characteristics of 5' NTR mutant viruses 5'D1 to
255 5'D11 was achieved by infecting SW13 cell cultures at an MOI of 0.01, and assessing
256 N protein production as a surrogate marker for HAZV gene expression by western
257 blotting at both 18 and 48 hpi time points (Fig 3C and D). At the 18 hpi time point,
258 representing a single infectious cycle, rescued viruses 5'D3 to 5'D7 exhibited
259 significantly reduced N protein expression compared to WT, as quantified by
260 densitometry of three independent infections (Fig 3E and F). This suggested these
261 viruses possessed a deficiency in an early stage of the life cycle, up to and including
262 S segment mRNA accumulation and subsequent N protein translation. At the 48 hpi
263 time point, the same viruses with the exception of 5'D4 and 5'D5 still showed reduced
264 N production compared to WT, suggesting that the influence of the deficiency was
265 maintained through subsequent rounds of infection.

266 The nucleotide alterations within mutants 5'D13 and 5'D12, which failed to
267 rescue, impinge upon PE1 and PE2, respectively, which confirms the critical role of
268 these S segment sequences in the HAZV multiplication cycle. In addition, the
269 significant drop in virus growth for the five viruses 5'D3 to 5'D7 revealed important
270 roles for the corresponding 50 deleted nucleotides, which together represents almost
271 half of the entire 5' NTR.

272 Taken together, these results show that any impingement on PE1 and PE2
273 within either 3' or 5' NTRs represents a severely debilitating or even lethal mutation,

and the 5' NTR is more sensitive to alteration that the 3' NTR, likely due to the presence of functionally-important sequences within this region.

The importance of PE2 nucleotide composition for virus viability. The results of the previous section showed that mutants 3'D6 and 3'D7 were viable but extremely unfit, and mutants 5'D12 and 5'D13 could not be rescued. Interestingly, for mutants 3'D7, 5'D12 and 5'D13, the altered nucleotides fall within PE2, the terminal-distal promoter region found to require, in major part, inter-terminal Watson-Crick base pairing for its promoter activity (25). The number of potential complementary inter-terminal parings within these three mutants differs; for 3'D7 it is just two (Fig 2H), for 5'D12 it is five (Fig 3G), and for 5'D13 it is three (Fig 3G). Taken together, these findings are consistent with the proposal that a high degree of complementary within PE2 is an important determinant of virus viability.

To further investigate the role of PE2 nucleotides during the complete HAZV infectious cycle, we designed plasmids to generate altered S segments in which the entire seven nucleotides that correspond to either 3' or 5' components of PE2 were cleanly deleted, yielding plasmids Delta 3'PE2 and Delta 5'PE2 respectively (Fig 4A). The alterations reduced the number of potential inter-terminal base pairs within the proposed PE2 region from seven to just two, and based on the finding that mutants 3'D7, 5'D12 and 5'D13 bearing partially-deleted PE2 regions were either barely- or non-viable, we predicted viruses Delta 3'PE2 and Delta 5'PE2 would be similarly unfit, or non-viable.

The corresponding altered plasmids were transfected into cells to attempt rescue, and although rescue of Delta 3'PE2 and Delta 5'PE2 viruses was achieved (Fig 4B), their resulting titres were extremely low (Fig 4C) at less than 200 viruses per

299 ml in transfected cell supernatants (Fig 4D). This outcome was entirely consistent with
300 the proposed important role of nucleotide complementarity in the functionality of PE2,
301 but nevertheless showed extensive complementarity was not an absolute necessity
302 for virus viability.

303 To further test the contribution of nucleotide sequence identity in the
304 functionality of PE2, we next designed plasmid G/C PE2 to generate an S segment in
305 which the overall inter-terminal complementarity of PE2 was unchanged, comprising
306 two A-U parings and five G-C pairings, but which possessed a novel sequence that
307 was not present in WT S, M or L segments (Fig 5A). The plasmid was transfected into
308 cells, and corresponding virus G/C PE2 was rescued at first attempt (Fig 5B) and
309 plaque assay of resulting supernatants revealed growth characteristics that were
310 indistinguishable from WT rescued alongside (Fig 5C and D). Taken together, these
311 findings are consistent with a scenario in which the base pairing potential of PE2 is
312 important rather than absolutely necessary, and furthermore does not depend on
313 specific sequence.

314

315 **PE2 represents an independent and modular *cis*-acting sequence signal.** Our
316 findings described above, and those of previous studies (25), highlight the importance
317 of PE2 and also show its signalling ability can be provided by multiple different
318 sequences. Taken together, these results suggest PE2 acts as an independent
319 module that provides its signalling ability without interaction with PE1 or any other
320 sequence signals elsewhere within the NTRs.

321 To test the independent signalling ability of PE2 in the context of the complete
322 HAZV replication cycle, we generated an S segment plasmid in which both 3' and 5'
323 portions of the M segment PE2 (Fig 6A) replaced the corresponding sequences of the

S segment (Fig 6B). This strategy allowed us to switch sequences that were entirely wild-type and thus known to be functional in their respective segment contexts. The resulting virus would thus possess an M segment PE2 surrounded by all other control sequences derived from the S segment.

The M-PE2 plasmid along with WT M and L segment-expressing plasmids were transfected into BSRT7 cells, and virus recovered at first attempt (Fig 6C), with a supernatant titre not significantly different than that of WT, indicating a high level of virus fitness (Fig 6D and E). This finding indicated that PE2 could be interchanged and still remain functional in an entirely different sequence context, thus implying the signalling ability of PE2 was independent from all other signalling nucleotides. Not surprisingly, viruses in which S segment PE2 nucleotides from either the 3' NTR or the 5' NTR alone were exchanged for the corresponding M segment PE2 sequences (3'M PE2 and 5'M PE2) could not be rescued, further reinforcing the dependence of inter-terminal interaction within PE2 for its function (Fig 6C-E).

DISCUSSION

By analogy with other bunyaviruses, the 3' and 5' NTRs of nairovirus S, M and L segments are expected to be multifunctional and perform critical functions in signalling multiple roles relating to viral RNA synthesis including transcription initiation, transcription termination, mRNA translation enhancement and RNA replication. However, it is possible that the NTRs participate in additional functions outside of RNA synthesis, for which virus fitness throughout the entire multiplication cycle must be considered.

Here, we performed for the first time a comprehensive deletion analysis of the entire nairovirus 3' and 5' NTRs, as well as a further dissection of the role of a discrete promoter element, PE2, all in the context of the entire nairovirus multiplication cycle. Our results revealed the 3' genomic NTR was remarkably tolerant of deletion; we detected no significant drop in rescued virus titre when deletions were made within the terminal distal 50 nucleotides, as represented by rescued viruses 3'D1 through 3'D5. These nucleotide changes also had no significant influence over virus multiplication at either 18 hpi or 48 hpi infection time points, suggesting no detectable involvement on virus multiplication within initially infected cells, and also no influence on the assembly, egress, infectivity and subsequent multiplication of virus in further cells. Interestingly however, deletions closer to the 3' genomic termini, as exemplified by mutant viruses 3'D6 and 3'D7 exhibited profound effects on virus fitness, with both these mutants being barely viable, and rescued with post transfection titres of around 10 viruses per ml. The deletion within mutant 3'D7 was within the previously identified conserved PE2, confirming the importance of this sequence element. However, the deletion in 3'D6 was outside of any previously identified promoter sequence elements, thus newly identifying critical nucleotides required for efficient virus growth. It is noteworthy that

of the ten nucleotides deleted within the 3’ NTR of 3’D6, five possess the potential to form inter-terminal Watson-Crick base pairings. Interestingly, three of these residues form a contiguous triplet of identical nucleotides, with GGG provided by the 3’ NTR and CCC provided by the corresponding positions within the 5’ NTR, and furthermore, this feature is also present in the corresponding location within M and L segments (GGG/CCC in L; AAA/UUU in M). These results show that the nucleotides that build up promoter regions are complex and comprise more than just PE1, PE2 and the intervening spacer.

In contrast to these findings, deletion analysis of the HAZV 5’ genomic NTR revealed mutant viruses 5’D3 to 5’D7 were significantly growth impaired, with the corresponding nucleotide sequences encompassing 50 nucleotides within the central region of the 5’ NTR. Growth at 18 hpi was significantly reduced compared to WT, with growth at 48 hpi following the same general trend. This suggested the influence of all the deleted residues was in virus multiplication rather than virion assembly, egress or infectivity. Mutants 5’D12 and 5’D13 could not be rescued, an outcome that was consistent with their corresponding deletions, which impinged on PE1 or PE2.

The reduced fitness and growth of mutants 5’D3 to 5’D7 suggested the corresponding deleted nucleotides play an important function in the virus multiplication cycle. Interestingly, the correlation we have determined between genome NTR deletion and virus fitness and growth are broadly similar to those observed for BUNV, for which the 3’ genomic NTR also exhibited considerable functional plasticity compared to the more-sensitive 5’ genomic NTR. Taken together, these findings suggest bunyavirus 5’ NTRs are more functionally critical than the 3’ end, a notion that is supported by the significant differences in 3’ and 5’ NTR lengths across all segments. Perhaps the most striking example of this is the HAZV L segment, for which

389 the 3’ NTR is 37 nucleotides long, whereas the 5’ NTR is nearly five times as long,
390 comprising 171 nucleotides. Bunyaviruses, such as the prototypic BUNV, have been
391 shown to eliminate nucleotides that are not beneficial to virus multiplication (28), and
392 so it is likely that these long 5’ NTRs do possess significant benefit to certain phases
393 of the multiplication cycle, and perhaps within certain hosts. Recent work with the
394 related segmented negative stranded RNA virus influenza virus has uncovered
395 additional roles of the NTRs including involvement in inter-segment interactions during
396 virus assembly, expression of short viral RNAs involved in modulating RdRp activity,
397 or in expressing RNAs that antagonize the host cell innate immune response (29–31).
398 The possibility that the long nairoviral NTRs perform similar roles has yet to be
399 investigated, and these studies provide a first step in this analysis by establishing a
400 framework of NTR functionality.

401 One role described for the bunyavirus 5’ NTR is in signalling the formation of
402 mRNA 3’ ends. For BUNV, the transcription termination signal resides within a central
403 position of the genomic 5’ NTR, and comprises the conserved hexanucleotide
404 sequence 3’-GUCGAC-5’ (12), and a similar motif is also proposed to act as a
405 transcription terminator for the related Rift Valley fever phlebovirus (32, 33). In BUNV,
406 the termination sequence is upstream of the mapped mRNA 3’ end (34), and also
407 adjacent to nucleotides that possess the ability to form stem loop secondary structure
408 that possesses translation-enhancing properties (14). Alignment of the HAZV S, M
409 and L segment 5’ NTRs fails to reveal similar sequences to either these bunyavirus-
410 specific termination signals, or the common poly (U) tract motif used by non-
411 segmented negative sense RNA viruses for 3’ poly (A) addition. Thus, it is entirely
412 possible that nairovirus 3’ mRNA end formation involves a novel mechanism, which
413 utilizes *cis*-acting sequence signals unrelated to those of other related viruses.

Our deletion analyses revealed the importance of the PE2 regions in the HAZV multiplication cycle, with complete or partial deletion of PE2 nucleotides having a significant influence on overall virus fitness and growth, in agreement with previous reporter analysis in the context of mini-genomes (25). Despite this, we showed that viruses with drastic changes to PE2 affecting both sequence and extent of complementarity were still viable and able to perform all aspects of the multiplication cycle, albeit with very poor fitness.

Our findings, along with those of others (25), strongly suggest that the role of PE2 is to drive nothing other than inter-terminal interactions mediated by canonical Watson-Crick pairings. Our finding that an alternate G/C-rich PE2 sequence, with no commonality to those within either S, M or L segments, is functionally equivalent to WT in all aspects of the multiplication cycle also agrees with this proposal (Fig 5), as does the ability of the M segment PE2 to function out of its canonical NTR context (Fig 6). However, it is important to note that Matsumoto and co-workers suggested the signal provided by PE2 depended not only on duplex formation, but also on the nucleotide sequence of this double stranded region. This conclusion was based on several variations of the PE2 sequence, with some providing low or undetectable reporter activity despite possessing perfect complementarity throughout the entire PE2 length. This observation prompted the suggestion that the duplex might be recognised by an RNA binding surface that is capable of distinguishing the base-composition of PE2, most likely located on the viral RdRp, perhaps to tether the RNP during transitional events required to reposition the 3' end of the RNA template from the outer RdRp surface into the RdRp active site. While the mutagenic analysis of PE2 performed here is not sufficiently extensive to definitively prove or disprove the question of PE2 sequence specificity, it is intriguing to note that the PE2 sequence we

439 engineered into the S segment of G/C PE2 (Fig 5) has no common sequence with the
440 WT S segment excepting the flanking A-U pairings, previously shown to be
441 dispensable. Therefore, if such a sequence specific dsRNA binding site exists, it must
442 also be capable of binding to this novel PE2 sequence within rHAZV G/C PE2, and
443 thus its nucleotide selectivity must be extremely low.

444 Achieving a detailed understanding of nairovirus molecular virology is very
445 much in its infancy, in part due to the extreme pathogenicity of the constituent
446 members of this group, and hopefully progress will accelerate with the use of both the
447 recent HAZV mini-genome (25) and virus rescue systems (26) that are now available,
448 and amenable to low containment level study.

449

MATERIALS AND METHODS

Cells and viruses. Baby hamster kidney derived BSR-T7 cells expressing T7 RNAP were maintained in Dulbecco's modified Eagle medium (DMEM) (Sigma Aldrich) supplemented with 2.5 % foetal bovine serum (FBS) (Invitrogen). Human adrenal cortex SW13 cells were maintained in DMEM containing 10% FBS. All media were supplemented with 100 U/ml penicillin and 100 μg/ml streptomycin and cultures were grown at 37 °C under an atmosphere of 5 % CO_2.

Plasmids and virus sequences. Plasmids pMK-RQ-S, pMK-RQ-M and pMK-RQ-L expressing the S, M and L segment antigenomic strands of HAZV strain JC280 were generated as previously described (26). We note that the sequence of the S segment used in the recently reported HAZV mini-genome system (25) differs from our JC280 sequence by a single nucleotide, at position 25 of the 3' NTR. Plasmid pCAG-T7pol was a gift from Ian Wickersham (Addgene plasmid #59926). Plasmids expressing altered S segments were generated using the Q5 Site Directed Mutagenesis kit (New England Biolabs) according to the manufacturer's instructions, and all mutant plasmid sequences confirmed via sequencing (Genewiz).

Virus rescue. The procedure for rescue of wild type and mutant HAZV has been previously described. Briefly, six-well plates with $1.5x10^5$ BSR-T7 cells/well in 2 ml DMEM supplemented with 2.5 % FBS were transfected 20-24 hours later with 1.2 μg of pMK-RQ-S, pMK-RQ-M, pMK-RQ-L and 0.6 μg pCAG-T7pol, using 2.5 μl Mirus TransIT-LT1 transfection reagent (Mirus Bio) per μg of DNA in 200 μl OPTI-MEM (Life Technologies). For recovery of HAZV mutants, the WT S segment-specific plasmid was replaced with the corresponding mutant plasmid. For each recovery, a control

transfection was set up in which transfection of pMK-RQ-L was omitted. Culture supernatants were collected at 120-hours post transfection. A 200 μl aliquot of the same supernatant was used to titre virus following transfection using a standard plaque assay protocol in duplicate. For each rescued virus, excepting 3'D7, 5'D12 and 5'D13, which were severely attenuated, RT-PCR analysis was used to confirm the expected mutant genotype, alongside control PCR amplifications in which RT was omitted.

Virus infections. Cultures of SW13 cells were infected with mutant and wild type recombinant HAZV at a specified multiplicity of infection (MOI) in serum-free DMEM at 37 °C. After 1 hour, the inoculum was removed and cells were washed in phosphate buffered saline (PBS) after which fresh DMEM containing 2.5 % FBS, 100 U/ml penicillin and 100 μg/ml streptomycin was then applied for the duration of the infection.

Western blotting. Cell lysates were prepared by washing monolayers in ice cold PBS followed by incubation in chilled RIPA buffer (150 mM sodium chloride, 1.0% NP-40 alternative, 0.1% SDS, 50 mM Tris, pH 8.0) with agitated for 2 minutes. Cell material was harvested by scraping and transferred to chilled Eppendorf tubes, after which lysates were centrifuged at 20,000 x g for 15 minutes, and the insoluble fraction discarded. SDS-gel loading buffer supplemented with DTT was added to the supernatant fraction prior to electrophoresis or storage at -20ºC. Proteins were separated on 12 % SDS polyacrylamide gels by electrophoresis and transferred to fluorescence compatible PVDF (FL-PVDF) membranes. HAZV-N antiserum generated as previously described was used to detect HAZV-N in combination with

fluorescently labelled anti-sheep secondary antibodies using the LiCor Odyssey Sa Infrared imaging system.

Virus titration. Determination of virus titre for assessment of rHAZV rescue growth characteristics was achieved through plaque assay, and were performed as previously described. Briefly, SW13 cells were seeded ($2x10^6$) into 75 cm^2 flasks 24 hours prior and used for the infection with wild type or mutant rHAZV at an MOI of 0.001. Supernatant was collected at various time points, serially-diluted, and then used to infect fresh SW13 cells in a 6-well plate. Following virus adsorption, the inoculum was removed and replaced with 1:1 2.5 % FBS DMEM and 1.6 % methylcellulose. Plates were incubated for a further 6 days prior to fixing with formaldehyde and staining with crystal violet to reveal plaques.

Extraction of viral RNA and RT-PCR. Viral RNA was first extracted from cell-free supernatant using the QIamp Viral RNA kit (Qiagen) and treated with DNase to remove any contaminating DNA prior to further purification using the RNeasy kit (Qiagen). A cDNA copy was generated using ProtoScript II Reverse Transcriptase (New England Biolabs) according to manufacturer's instructions alongside a control in which the Reverse Transcriptase was omitted. PCR amplification of an ≈500 bp fragment using primers specific to the HAZV S segment was achieved using the Q5 High Fidelity Polymerase (New England Biolabs). PCR product was resolved on a 1 % agarose gel containing 0.01 % SYBR Safe (ThermoFisher) and sequenced (Genewiz).

ACKNOWLEDGEMENTS

This work was funded by a Public Health England PhD studentship to JF, an EU Marie Skłodowska-Curie Actions (MSCA) Innovative Training Network (ITN): H2020- MSCA-ITN-2016, grant No 721367 to BAR. DFM was self-funded. JNB, JF and DFM conceptualized the study, JF, DFM and BAR performed the experimental investigation, JNB wrote the original draft, and all other authors reviewed and edited the manuscript. JNB supervised the core team, provided management and coordination of activities and acquired financial support.

REFERENCES

1. Abudurexiti A, Adkins S, Alioto D, Alkhovsky S V, Avšič-Županc T, Ballinger MJ, Bente DA, Beer M, Bergeron É, Blair CD, Briese T, Buchmeier MJ, Burt FJ, Calisher CH, Cháng C, Charrel RN, Choi IR, Clegg JCS, de la Torre JC, de Lamballerie X, Dèng F, Di Serio F, Digiaro M, Drebot MA, Duàn X, Ebihara H, Elbeaino T, Ergünay K, Fulhorst CF, Garrison AR, Gāo GF, Gonzalez J-PJ, Groschup MH, Günther S, Haenni A-L, Hall RA, Hepojoki J, Hewson R, Hú Z, Hughes HR, Jonson MG, Junglen S, Klempa B, Klingström J, Kòu C, Laenen L, Lambert AJ, Langevin SA, Liu D, Lukashevich IS, Luò T, Lǚ C, Maes P, de Souza WM, Marklewitz M, Martelli GP, Matsuno K, Mielke-Ehret N, Minutolo M, Mirazimi A, Moming A, Mühlbach H-P, Naidu R, Navarro B, Nunes MRT, Palacios G, Papa A, Pauvolid-Corrêa A, Pawęska JT, Qiáo J, Radoshitzky SR, Resende RO, Romanowski V, Sall AA, Salvato MS, Sasaya T, Shěn S, Shí X, Shirako Y, Simmonds P, Sironi M, Song J-W, Spengler JR, Stenglein MD, Sū Z, Sūn S, Táng S, Turina M, Wáng B, Wáng C, Wáng H, Wáng J, Wèi T, Whitfield AE, Zerbini FM, Zhāng J, Zhāng L, Zhāng Y, Zhang Y-Z, Zhāng Y, Zhou X, Zhū L, Kuhn JH. 2019. Taxonomy of the order Bunyavirales: update 2019. Arch Virol 164:1949–1965.
2. Davies FG. 1997. Nairobi sheep disease. Parassitologia 39:95–8.
3. Messina JP, Pigott DM, Golding N, Duda KA, Brownstein JS, Weiss DJ, Gibson H, Robinson TP, Gilbert M, William Wint GR, Nuttall PA, Gething PW, Myers MF, George DB, Hay SI. 2015. The global distribution of Crimean-Congo hemorrhagic fever. Trans R Soc Trop Med Hyg 109:503–13.
4. Negredo A, de la Calle-Prieto F, Palencia-Herrejón E, Mora-Rillo M, Astray-Mochales J, Sánchez-Seco MP, Bermejo Lopez E, Menárguez J, Fernández-

560 Cruz A, Sánchez-Artola B, Keough-Delgado E, Ramírez de Arellano E, Lasala
561 F, Milla J, Fraile JL, Ordobás Gavín M, Martinez de la Gándara A, López
562 Perez L, Diaz-Diaz D, López-García MA, Delgado-Jimenez P, Martín-Quirós A,
563 Trigo E, Figueira JC, Manzanares J, Rodriguez-Baena E, Garcia-Comas L,
564 Rodríguez-Fraga O, García-Arenzana N, Fernández-Díaz M V, Cornejo VM,
565 Emmerich P, Schmidt-Chanasit J, Arribas JR, Crimean Congo Hemorrhagic
566 Fever@Madrid Working Group. 2017. Autochthonous Crimean-Congo
567 Hemorrhagic Fever in Spain. N Engl J Med 377:154–161.
568 5. Surtees R, Dowall SD, Shaw A, Armstrong S, Hewson R, Carroll MW,
569 Mankouri J, Edwards TA, Hiscox JA, Barr JN. 2016. Heat Shock Protein 70
570 Family Members Interact with Crimean-Congo Hemorrhagic Fever Virus and
571 Hazara Virus Nucleocapsid Proteins and Perform a Functional Role in the
572 Nairovirus Replication Cycle. J Virol 90:9305–16.
573 6. Surtees R, Ariza A, Punch EK, Trinh CH, Dowall SD, Hewson R, Hiscox JA,
574 Barr JN, Edwards TA. 2015. The crystal structure of the Hazara virus
575 nucleocapsid protein. BMC Struct Biol 15:24.
576 7. Wang W, Liu X, Wang X, Dong H, Ma C, Wang J, Liu B, Mao Y, Wang Y, Li T,
577 Yang C, Guo Y. 2015. Structural and Functional Diversity of Nairovirus-
578 Encoded Nucleoproteins. J Virol 89:11740–9.
579 8. Barnwal B, Karlberg H, Mirazimi A, Tan Y-J. 2016. The Non-structural Protein
580 of Crimean-Congo Hemorrhagic Fever Virus Disrupts the Mitochondrial
581 Membrane Potential and Induces Apoptosis. J Biol Chem 291:582–92.
582 9. Barr JN, Elliott RM, Dunn EF, Wertz GW. 2003. Segment-specific terminal
583 sequences of Bunyamwera bunyavirus regulate genome replication. Virology
584 311:326–38.

585 10. Barr JN, Wertz GW. 2004. Bunyamwera bunyavirus RNA synthesis requires
586 cooperation of 3'- and 5'-terminal sequences. J Virol 78:1129–38.
587 11. Barr JN, Wertz GW. 2005. Role of the conserved nucleotide mismatch within
588 3'- and 5'-terminal regions of Bunyamwera virus in signaling transcription. J
589 Virol 79:3586–94.
590 12. Barr JN, Rodgers JW, Wertz GW. 2006. Identification of the Bunyamwera
591 bunyavirus transcription termination signal. J Gen Virol 87:189–98.
592 13. Mazel-Sanchez B, Elliott RM. 2012. Attenuation of bunyamwera
593 orthobunyavirus replication by targeted mutagenesis of genomic untranslated
594 regions and creation of viable viruses with minimal genome segments. J Virol
595 86:13672–8.
596 14. Blakqori G, van Knippenberg I, Elliott RM. 2009. Bunyamwera orthobunyavirus
597 S-segment untranslated regions mediate poly(A) tail-independent translation. J
598 Virol 83:3637–46.
599 15. Kohl A, Lowen AC, Léonard VHJ, Elliott RM. 2006. Genetic elements
600 regulating packaging of the Bunyamwera orthobunyavirus genome. J Gen Virol
601 87:177–87.
602 16. Lowen AC, Elliott RM. 2005. Mutational analyses of the nonconserved
603 sequences in the Bunyamwera Orthobunyavirus S segment untranslated
604 regions. J Virol 79:12861–70.
605 17. Lowen AC, Boyd A, Fazakerley JK, Elliott RM. 2005. Attenuation of bunyavirus
606 replication by rearrangement of viral coding and noncoding sequences. J Virol
607 79:6940–6.
608 18. Kohl A, Bridgen A, Dunn E, Barr JN, Elliott RM. 2003. Effects of a point
609 mutation in the 3' end of the S genome segment of naturally occurring and

610 engineered Bunyamwera viruses. J Gen Virol 84:789–93.
611 19. Gerlach P, Malet H, Cusack S, Reguera J. 2015. Structural Insights into
612 Bunyavirus Replication and Its Regulation by the vRNA Promoter. Cell
613 161:1267–79.
614 20. Kohl A, Dunn EF, Lowen AC, Elliott RM. 2004. Complementarity, sequence
615 and structural elements within the 3' and 5' non-coding regions of the
616 Bunyamwera orthobunyavirus S segment determine promoter strength. J Gen
617 Virol 85:3269–78.
618 21. Barr JN, Rodgers JW, Wertz GW. 2005. The Bunyamwera virus mRNA
619 transcription signal resides within both the 3' and the 5' terminal regions and
620 allows ambisense transcription from a model RNA segment. J Virol 79:12602–
621 7.
622 22. Ariza A, Tanner SJ, Walter CT, Dent KC, Shepherd DA, Wu W, Matthews S V.,
623 Hiscox JA, Green TJ, Luo M, Elliott RM, Fooks AR, Ashcroft AE, Stonehouse
624 NJ, Ranson NA, Barr JN, Edwards TA. 2013. Nucleocapsid protein structures
625 from orthobunyaviruses reveal insight into ribonucleoprotein architecture and
626 RNA polymerization. Nucleic Acids Res 41:5912–5926.
627 23. Reguera J, Malet H, Weber F, Cusack S. 2013. Structural basis for
628 encapsidation of genomic RNA by La Crosse Orthobunyavirus nucleoprotein.
629 Proc Natl Acad Sci U S A 110:7246–51.
630 24. Mohl B-P, Barr JN. 2009. Investigating the specificity and stoichiometry of RNA
631 binding by the nucleocapsid protein of Bunyamwera virus. RNA 15:391–9.
632 25. Matsumoto Y, Ohta K, Kolakofsky D, Nishio M. 2019. A Minigenome Study of
633 Hazara Nairovirus Genomic Promoters. J Virol 93.
634 26. Fuller J, Surtees RA, Slack GS, Mankouri J, Hewson R, Barr JN. 2019.

635 Rescue of Infectious Recombinant Hazara Nairovirus from cDNA Reveals the
636 Nucleocapsid Protein DQVD Caspase Cleavage Motif Performs an Essential
637 Role other than Cleavage. J Virol 93.
638 27. Elliott RM, Wilkie ML. 1986. Persistent infection of Aedes albopictus C6/36
639 cells by Bunyamwera virus. Virology 150:21–32.
640 28. Shi X, van Mierlo JT, French A, Elliott RM. 2010. Visualizing the Replication
641 Cycle of Bunyamwera Orthobunyavirus Expressing Fluorescent Protein-
642 Tagged Gc Glycoprotein. J Virol 84:8460–8469.
643 29. Dadonaite B, Gilbertson B, Knight ML, Trifkovic S, Rockman S, Laederach A,
644 Brown LE, Fodor E, Bauer DL V. 2019. The structure of the influenza A virus
645 genome. Nat Microbiol 4:1781–1789.
646 30. Te Velthuis AJW, Long JC, Bauer DL V, Fan RLY, Yen H-L, Sharps J, Siegers
647 JY, Killip MJ, French H, Oliva-Martín MJ, Randall RE, de Wit E, van Riel D,
648 Poon LLM, Fodor E. 2018. Mini viral RNAs act as innate immune agonists
649 during influenza virus infection. Nat Microbiol 3:1234–1242.
650 31. Perez JT, Varble A, Sachidanandam R, Zlatev I, Manoharan M, García-Sastre
651 A, TenOever BR. 2010. Influenza A virus-generated small RNAs regulate the
652 switch from transcription to replication. Proc Natl Acad Sci U S A 107:11525–
653 30.
654 32. Albariño CG, Bird BH, Nichol ST. 2007. A shared transcription termination
655 signal on negative and ambisense RNA genome segments of Rift Valley fever,
656 sandfly fever Sicilian, and Toscana viruses. J Virol 81:5246–56.
657 33. Lara E, Billecocq A, Leger P, Bouloy M. 2011. Characterization of wild-type
658 and alternate transcription termination signals in the Rift Valley fever virus
659 genome. J Virol 85:12134–45.

34. Jin H, Elliott RM. 1993. Characterization of Bunyamwera virus S RNA that is transcribed and replicated by the L protein expressed from recombinant vaccinia virus. J Virol 67:1396–404.

FIGURE LEGENDS

Figure 1. Schematic showing nairovirus S, M and L segments, the proposed S segment promoter structure and deletions made within S segment NTRs for attempted rescue. A) Schematic of HAZV S, M and L genome segments with lengths of the respective NTRs shown. B) Nucleotide sequences of the first 40 terminal-proximal nucleotides of 3' and 5' NTRs of the HAZV S segment genome, shown with termini aligned and with complementary nucleotides marked with an asterisk. Proposed promoter elements PE1 and PE2 comprising complementary nucleotides from both 3' and 5' NTRs are shown as shaded boxes. C) Shaded regions represent successive 10-nucleotide long blocks that were deleted within corresponding S segments, and subsequently used to attempt virus rescue with wild-type HAZV M and L segments. Position of nucleotides included within proposed PE1 and PE2 are shown for reference.

Figure 2. Rescue of recombinant HAZV with S segments bearing successive 10 nucleotide deletions in the 3' NTR. A) Successful rescue of recombinant wild-type HAZV from cDNAs expressing S, M and L segments indicated by western blot analysis of transfected BSRT7 cell lysates using HAZV N protein antisera. The mock (M) lane represents un-transfected lysates, control (Ctrl) lane indicates transfected cells in which the L segment-expressing cDNA was omitted. B) Titres of rescued recombinant viruses from initial transfection cultures was determined by crystal violet stained plaque assay, with a single well of each 3' NTR deletion mutant shown (not equivalent dilutions), with resulting titres represented graphically in C). D) Growth properties of mutant viruses bearing 3' NTR deletions as determined by western blot analysis using

689 HAZV N protein antisera of SW13 cultures infected at an MOI of 0.01. Lysates were
690 harvested at 18-hours and E), 48-hours post infection time points, with N protein
691 abundance determined by densitometry analysis of three independent infections,
692 shown in F) and G). One sample t-test was performed to determine statistically
693 significant differences between mutants and WT virus. ns: not significant, *: p-
694 value<0.1. H) Nucleotide alignment of genomic 3' and 5' NTRs of highly-attenuated
695 mutants 3'D6 and 3'D7, with complementary nucleotides marked with an asterisk, and
696 PE1 and PE2 promoter elements shown as shaded boxes. Open boxes on left-hand
697 segment schematics show deleted nucleotides, and red nucleotides on the right-hand
698 segment schematics show subsequent alterations in the context of the terminal
699 duplex.
700
701 **Figure 3. Rescue of recombinant HAZV with S segments bearing successive 10**
702 **nucleotide deletions in the 5' NTR.** A) Titres of rescued recombinant viruses from
703 initial transfection cultures were determined by crystal violet stained plaque assay,
704 with a single well of each 5' NTR deletion mutant shown (not equivalent dilutions), and
705 resulting titres tabulated in B). Growth properties of mutant viruses bearing 5' NTR
706 deletions as determined by western blot analysis using HAZV N protein antisera of
707 SW13 cultures infected at an MOI of 0.01. Lysates were harvested at both C), 18-
708 hours and D), 48-hours post infection, with N protein abundance determined by
709 densitometric analysis of western blots representing three independent infections,
710 shown in E) and F), respectively. One sample t-test was performed to determine
711 statistically significant differences between mutants and WT virus; ns: not significant,
712 *: p-value<0.1, **: p-value<0.01, ***: p-value<0.001. G) Nucleotide alignment of
713 genomic 3' and 5' NTRs of highly-attenuated mutants 5'D12 and 5'D13, with

complementary nucleotides marked with an asterisk, and PE1 and PE2 promoter elements shown as shaded boxes. Open boxes on left-hand segment schematics show nucleotides to be deleted, and red nucleotides on the right-hand segment schematics show subsequent alterations in the context of the terminal duplex.

Figure 4. The effect of deletion of S segment PE2 on HAZV viability. A) Nucleotide sequence alignment of genomic 3' and 5' NTRs of wild type and mutant HAZV S segments bearing changes within PE2, with complementary nucleotides marked with an asterisk, and PE1 and PE2 promoter elements shown as shaded boxes. Open boxes on left-hand segment schematics show nucleotides to be deleted, and red nucleotides on the right-hand segment schematics show subsequent alterations in the context of the terminal duplex. B) Successful rescue of recombinant HAZV indicated by western blot analysis of transfected cell lysates using HAZV N protein antisera. The mock (M) lane represents un-transfected lysates, control (Ctrl) lane indicates transfected cells in which the L segment-expressing cDNA was omitted. C) Titres of rescued recombinant Delta 3'PE2 and Delta 5'PE2 viruses from initial transfection cultures was determined by crystal violet stained plaque assay alongside wild type, with a single well of both viruses shown (not equivalent dilutions), with resulting titres represented graphically in D).

Figure 5. Nucleotide complementarity of PE2 is a key determinant of HAZV viability. A) Nucleotide sequence alignment of genomic 3' and 5' NTRs of wild type and G/C mutant S segments, with complementary nucleotides marked with an asterisk, and PE1 and PE2 promoter elements shown as shaded boxes. Open boxes on left-hand segment schematics show nucleotides to be deleted, and red nucleotides

on the right-hand segment schematics show subsequent alterations in the context of the terminal duplex. B) Successful rescue of recombinant HAZV G/C mutant indicated by western blot analysis of transfected cell lysates using HAZV N protein antisera. The mock (M) lane represents un-transfected lysates, control (Ctrl) lane indicates transfected cells in which the L segment-expressing cDNA was omitted. C) Titres of rescued recombinant G/C HAZV from initial transfection cultures was determined by crystal violet stained plaque assay alongside wild type, with a single well of both viruses shown (equivalent dilutions), with resulting mean titres from two independent rescue experiments represented graphically in D). Paired t-test was performed to determine statistically significant differences between mutant and WT virus. ns: not significant.

Figure 6. S segment PE2 sequences can be functionally-replaced with those of the M segment. A) Nucleotide sequence alignment of genomic 3' and 5' NTRs of HAZV S and M segments, with complementary nucleotides marked with an asterisk, and PE1 and PE2 promoter elements shown as shaded boxes. Open boxes on the left-hand S segment schematic show nucleotides to be deleted. B) Nucleotide alignment of genomic 3' and 5' NTRs of HAZV S segments incorporating M segment PE2 sequences, with M segment derived nucleotides shown in red. C) Successful rescue of recombinant M PE2 indicated by western blot analysis of transfected cell lysates using HAZV N protein antisera. The mock (M) lane represents un-transfected lysates, control (Ctrl) lane indicates transfected cells in which the L segment-expressing cDNA was omitted. D) Titres of rescued recombinant HAZV mutants from initial transfection cultures was determined by crystal violet stained plaque assay alongside wild type, with a single well of both viruses shown (not equivalent dilutions),

764 with resulting titres represented graphically in E). Paired t-test was performed to
765 determine statistically significant differences between mutant and WT virus (ns: not
766 significant).
767

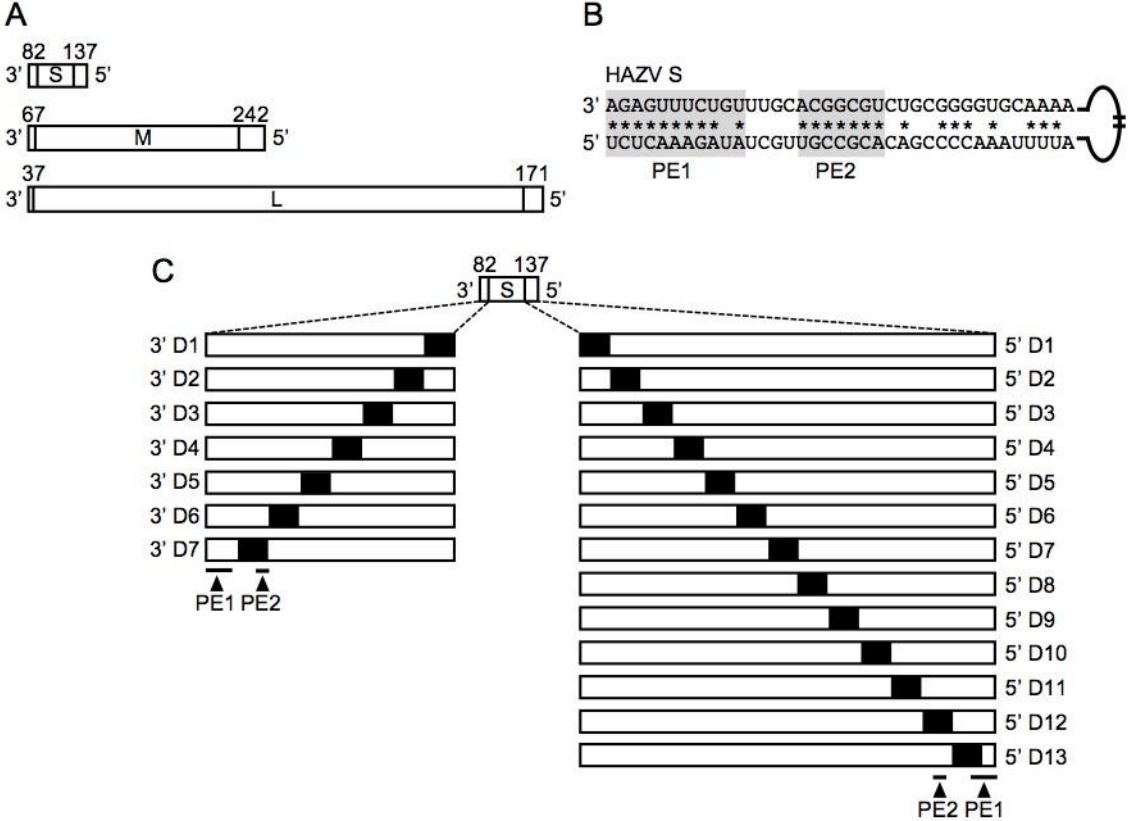
A
82 137
3' S 5'
67 242
3' M 5'
37 171
3' L 5'
B
HAZV S
3' AGAGUUUCUGUUUGCACGGCGUCUGCGGGGUGCAAAA
5' UCUCAAAGAUAUCGUUGCCGCACAGCCCCAAAUUUUA
PE1
PE2
C
82 137
3' S 5'
3' D1
3' D2
3' D3
3' D4
3' D5
3' D6
3' D7
PE1 PE2
5' D1
5' D2
5' D3
5' D4
5' D5
5' D6
5' D7
5' D8
5' D9
5' D10
5' D11
5' D12
5' D13
PE2 PE1

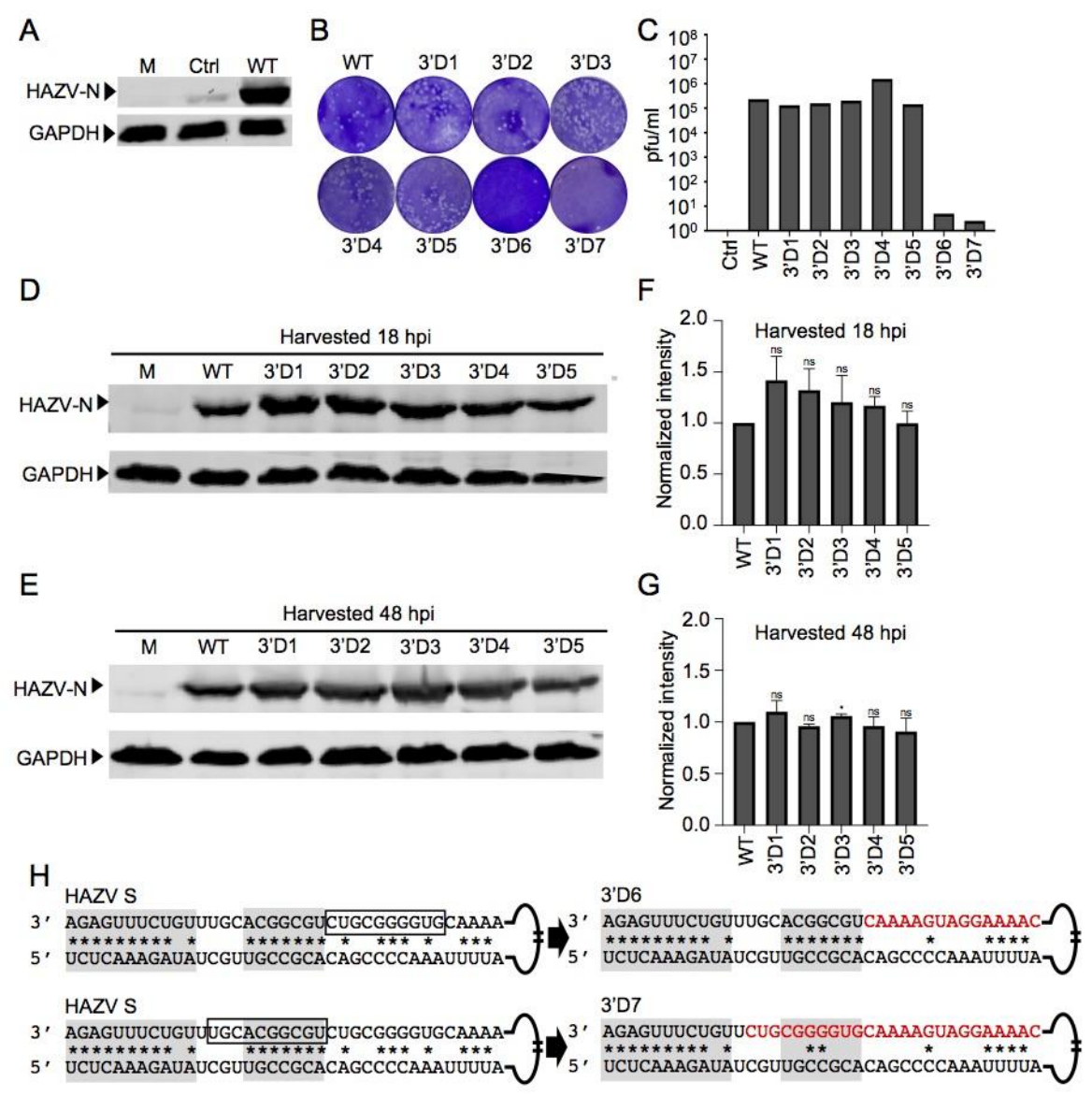
A
M
Ctrl
WT
HAZV-N
GAPDH
B
WT
3'D1
3'D2
3'D3
3'D4
3'D5
3'D6
3'D7
C
pfu/ml
Ctrl
WT
3'D1
3'D2
3'D3
3'D4
3'D5
3'D6
3'D7
D
Harvested 18 hpi
M
WT
3'D1
3'D2
3'D3
3'D4
3'D5
HAZV-N
GAPDH
F
Harvested 18 hpi
Normalized intensity
ns
WT
3'D1
3'D2
3'D3
3'D4
3'D5
E
Harvested 48 hpi
M
WT
3'D1
3'D2
3'D3
3'D4
3'D5
HAZV-N
GAPDH
G
Harvested 48 hpi
Normalized intensity
ns
WT
3'D1
3'D2
3'D3
3'D4
3'D5
H
HAZV S
3'D6
HAZV S
3'D7

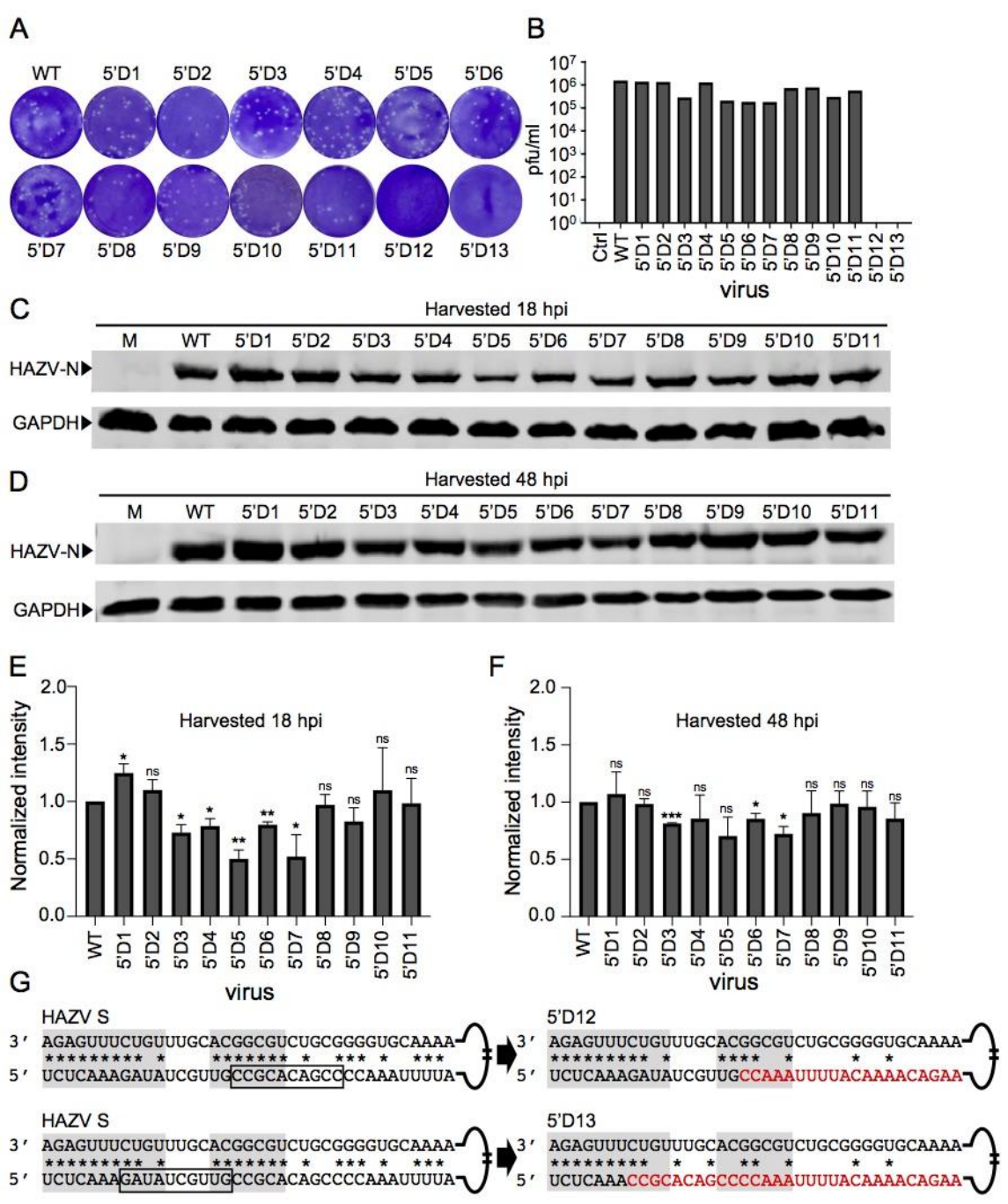
A
WT
5'D1
5'D2
5'D3
5'D4
5'D5
5'D6
5'D7
5'D8
5'D9
5'D10
5'D11
5'D12
5'D13
B
pfu/ml
virus
Ctrl
C
Harvested 18 hpi
M
HAZV-N
GAPDH
D
Harvested 48 hpi
E
Harvested 18 hpi
Normalized intensity
F
Harvested 48 hpi
G
HAZV S
5'D12
5'D13

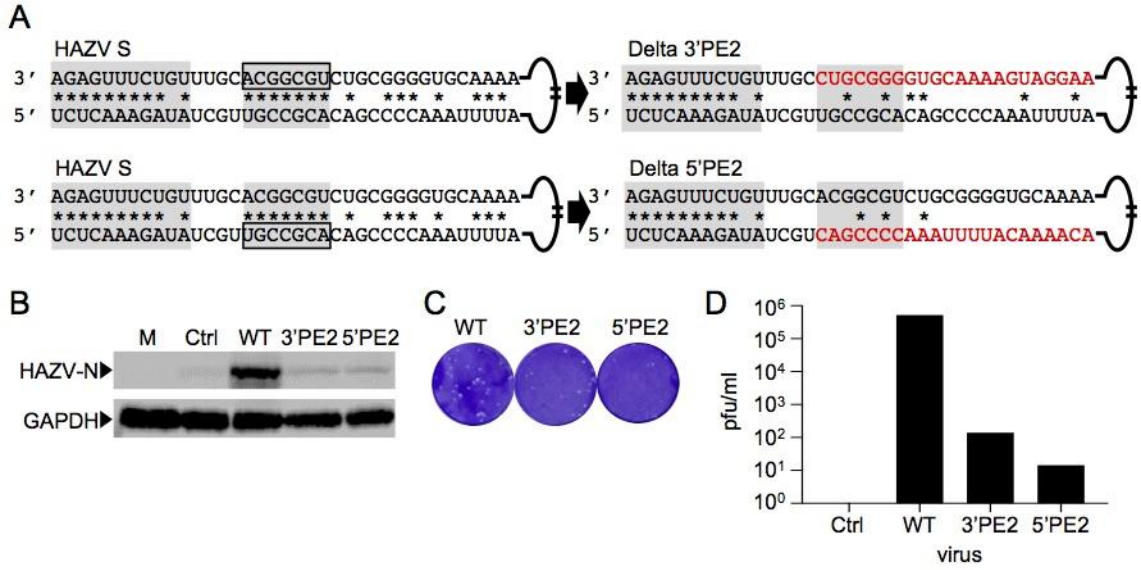
A
HAZV S
3′ AGAGUUUCUGUUUGCACGGCGUCUGCGGGGUGCAAAA
5′ UCUCAAAGAUAUCGUUGCCGCACAGCCCCAAAUUUUA
Delta 3′PE2
3′ AGAGUUUCUGUUUGCCUGCGGGGUGCAAAAGUAGGAA
5′ UCUCAAAGAUAUCGUUGCCGCACAGCCCCAAAUUUUA
HAZV S
3′ AGAGUUUCUGUUUGCACGGCGUCUGCGGGGUGCAAAA
5′ UCUCAAAGAUAUCGUUGCCGCACAGCCCCAAAUUUUA
Delta 5′PE2
3′ AGAGUUUCUGUUUGCACGGCGUCUGCGGGGUGCAAAA
5′ UCUCAAAGAUAUCGUCAGCCCCAAAUUUUACAAAACA
B
M Ctrl WT 3′PE2 5′PE2
HAZV-N
GAPDH
C
WT 3′PE2 5′PE2
D
pfu/ml
10^6 10^5 10^4 10^3 10^2 10^1 10^0
Ctrl WT 3′PE2 5′PE2
virus

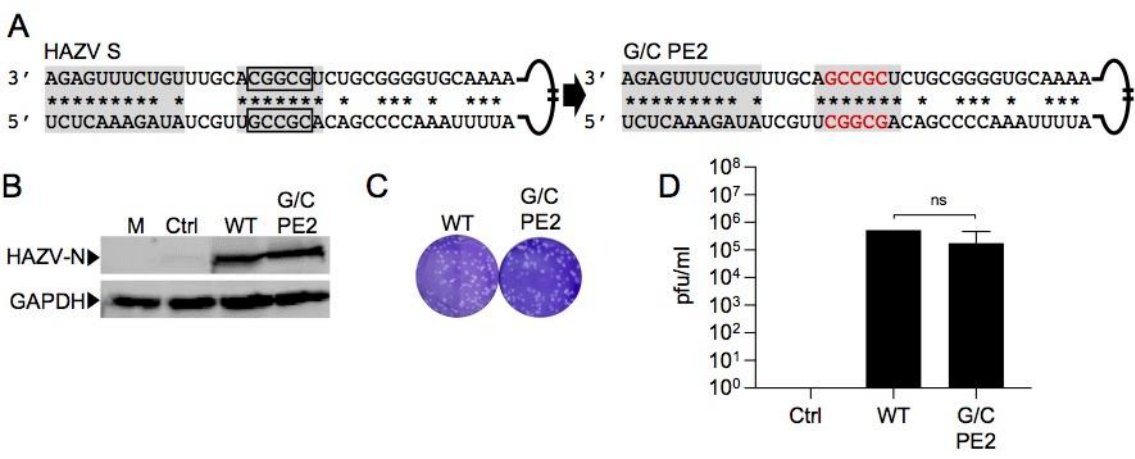
A
HAZV S
3′ AGAGUUUCUGUUUGCACGGCGUCUGCGGGGUGCAAAA
5′ UCUCAAAGAUAUCGUUGCCGCGACAGCCCCAAAUUUUA
G/C PE2
3′ AGAGUUUCUGUUUGCAGCCGCUCUGCGGGGUGCAAAA
5′ UCUCAAAGAUAUCGUUCGGCGACAGCCCCAAAUUUUA
B
M
Ctrl
WT
G/C PE2
HAZV-N
GAPDH
C
WT
G/C PE2
D
pfu/ml
ns
Ctrl
WT
G/C PE2

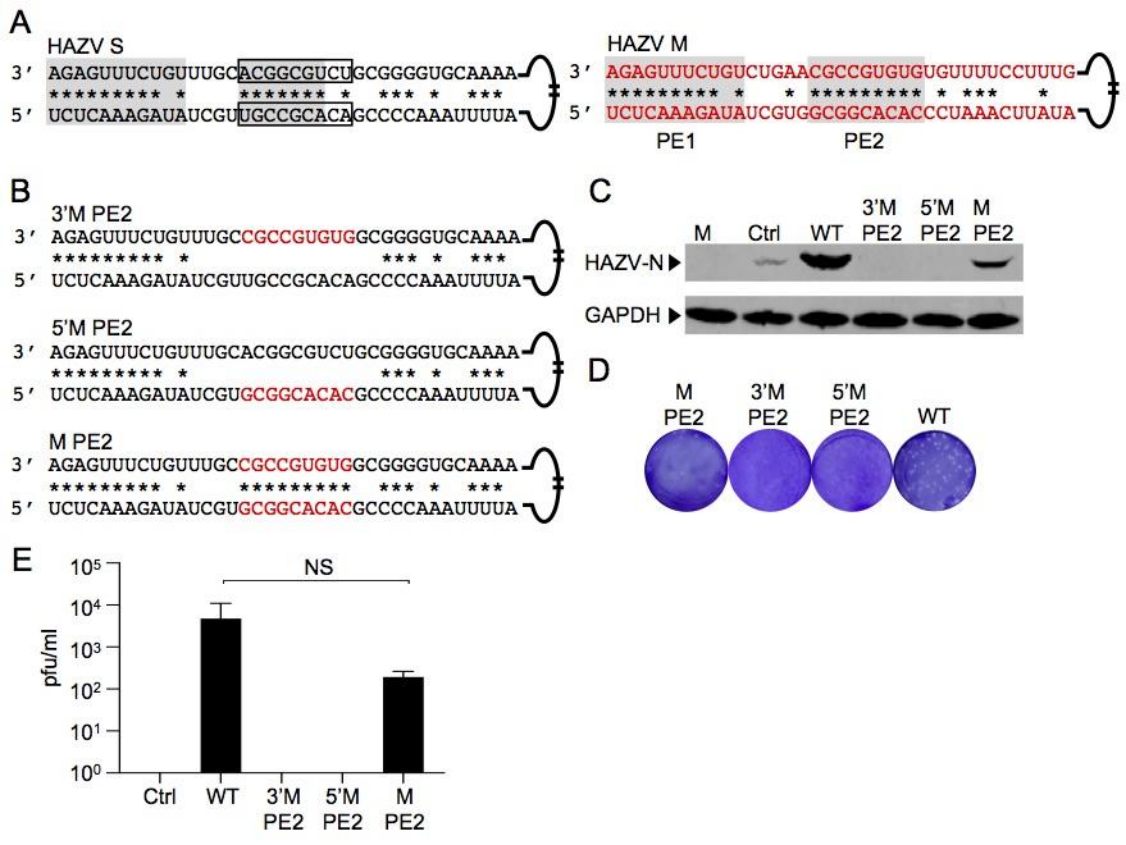
A
HAZV S
3′ AGAGUUUCUGUUUGCACGGCGUCUGCGGGGUGCAAAA
5′ UCUCAAAGAUAUCGUUGCCGCACAGCCCCAAAUUUUA
HAZV M
3′ AGAGUUUCUGUCUGAACGCCGUGUGUGUUUUCCUUUG
5′ UCUCAAAGAUAUCGUGGCGGCACACCCUAAACUUAUA
PE1
PE2
B
3′M PE2
3′ AGAGUUUCUGUUUGCCGCCGUGUGGCGGGGUGCAAAA
5′ UCUCAAAGAUAUCGUUGCCGCACAGCCCCAAAUUUUA
5′M PE2
3′ AGAGUUUCUGUUUGCACGGCGUCUGCGGGGUGCAAAA
5′ UCUCAAAGAUAUCGUGCGGCACACGCCCCAAAUUUUA
M PE2
3′ AGAGUUUCUGUUUGCCGCCGUGUGGCGGGGUGCAAAA
5′ UCUCAAAGAUAUCGUGCGGCACACGCCCCAAAUUUUA
C
M
Ctrl
WT
3′M PE2
5′M PE2
M PE2
HAZV-N
GAPDH
D
M PE2
3′M PE2
5′M PE2
WT
E
NS
pfu/ml
10^5
10^4
10^3
10^2
10^1
10^0
Ctrl
WT
3′M PE2
5′M PE2
M PE2

A

3′WT
AGAGUUUCUGUUUGUACGGCGUCUGCGGGGUGCAAAAGUAGGAAAACUCUCGUUUUGGCCAGCGGAGUGUUGUAGUCGCUCU*start*

3′D1
AGAGUUUCUGUUUGUACGGCGUCUGCGGGGUGCAAAAGUAGGAAAACUCUCGUUUUGGCCAGCGGAGUGUUG----------*start*

3′D2
AGAGUUUCUGUUUGUACGGCGUCUGCGGGGUGCAAAAGUAGGAAAACUCUCGUUUUGGCCAG----------UAGUCGCUCU*start*

3′D3
AGAGUUUCUGUUUGUACGGCGUCUGCGGGGUGCAAAAGUAGGAAAACUCUCG----------CGGAGUGUUGUAGUCGCUCU*start*

3′D4
AGAGUUUCUGUUUGUACGGCGUCUGCGGGGUGCAAAAGUAGG----------UUUUGGCCAGCGGAGUGUUGUAGUCGCUCU*start*

3′D5
AGAGUUUCUGUUUGUACGGCGUCUGCGGGGUG----------AAAACUCUCGUUUUGGCCAGCGGAGUGUUGUAGUCGCUCU*start*

3′D6
AGAGUUUCUGUUUGUACGGCGU----------CAAAAGUAGGAAAACUCUCGUUUUGGCCAGCGGAGUGUUGUAGUCGCUCU*start*

3′D7
AGAGUUUCUGUU----------CUGCGGGGUGCAAAAGUAGGAAAACUCUCGUUUUGGCCAGCGGAGUGUUGUAGUCGCUCU*start*

B

5′WT
UCUCAAAGAUAUCGUUGCCGCACAGCCCCAAAUUUUACAAAACAGAAUAGAAUAAGAAUGAAAGUAAGAAUAGAAGCAAAGCAAU
GCAGAAGAAAAACAGCAGUAGAGAUGUGUUGGCAGUGAACCUAGCCGCAAUC*stop*

5′D1
UCUCAAAGAUAUCGUUGCCGCACAGCCCCAAAUUUUACAAAACAGAAUAGAAUAAGAAUGAAAGUAAGAAUAGAAGCAAAGCAAU
GCAGAAGAAAAACAGCAGUAGAGAUGUGUUGGCAGUGAACCU----------*stop*

5′D2
UCUCAAAGAUAUCGUUGCCGCACAGCCCCAAAUUUUACAAAACAGAAUAGAAUAAGAAUGAAAGUAAGAAUAGAAGCAAAGCAAU
GCAGAAGAAAAACAGCAGUAGAGAUGUGUUGG----------AGCCGCAAUC*stop*

5′D3
UCUCAAAGAUAUCGUUGCCGCACAGCCCCAAAUUUUACAAAACAGAAUAGAAUAAGAAUGAAAGUAAGAAUAGAAGCAAAGCAAU
GCAGAAGAAAAACAGCAGUAGA----------CAGUGAACCUAGCCGCAAUC*stop*

5′D4
UCUCAAAGAUAUCGUUGCCGCACAGCCCCAAAUUUUACAAAACAGAAUAGAAUAAGAAUGAAAGUAAGAAUAGAAGCAAAGCAAU
GCAGAAGAAAAA----------GAUGUGUUGGCAGUGAACCUAGCCGCAAUC*stop*

5′D5
UCUCAAAGAUAUCGUUGCCGCACAGCCCCAAAUUUUACAAAACAGAAUAGAAUAAGAAUGAAAGUAAGAAUAGAAGCAAAGCAAU
GC----------CAGCAGUAGAGAUGUGUUGGCAGUGAACCUAGCCGCAAUC*stop*

5′D6
UCUCAAAGAUAUCGUUGCCGCACAGCCCCAAAUUUUACAAAACAGAAUAGAAUAAGAAUGAAAGUAAGAAUAGAAGC--------
--AGAAGAAAAACAGCAGUAGAGAUGUGUUGGCAGUGAACCUAGCCGCAAUC*stop*

5′D7
UCUCAAAGAUAUCGUUGCCGCACAGCCCCAAAUUUUACAAAACAGAAUAGAAUAAGAAUGAAAGUAA----------AAAGCAAU
GCAGAAGAAAAACAGCAGUAGAGAUGUGUUGGCAGUGAACCUAGCCGCAAUC*stop*

5′D8
UCUCAAAGAUAUCGUUGCCGCACAGCCCCAAAUUUUACAAAACAGAAUAGAAUAAGA----------GAAUAGAAGCAAAGCAAU
GCAGAAGAAAAACAGCAGUAGAGAUGUGUUGGCAGUGAACCUAGCCGCAAUC*stop*

5′D9
UCUCAAAGAUAUCGUUGCCGCACAGCCCCAAAUUUUACAAAACAGAA----------AUGAAAGUAAGAAUAGAAGCAAAGCAAU
GCAGAAGAAAAACAGCAGUAGAGAUGUGUUGGCAGUGAACCUAGCCGCAAUC*stop*

5′D10
UCUCAAAGAUAUCGUUGCCGCACAGCCCCAAAUUUUA----------UAGAAUAAGAAUGAAAGUAAGAAUAGAAGCAAAGCAAU
GCAGAAGAAAAACAGCAGUAGAGAUGUGUUGGCAGUGAACCUAGCCGCAAUC*stop*

5′D11
UCUCAAAGAUAUCGUUGCCGCACAGCC----------CAAAACAGAAUAGAAUAAGAAUGAAAGUAAGAAUAGAAGCAAAGCAAU
GCAGAAGAAAAACAGCAGUAGAGAUGUGUUGGCAGUGAACCUAGCCGCAAUC*stop*

5′D12
UCUCAAAGAUAUCGUUG----------CCAAAUUUUACAAAACAGAAUAGAAUAAGAAUGAAAGUAAGAAUAGAAGCAAAGCAAU
GCAGAAGAAAAACAGCAGUAGAGAUGUGUUGGCAGUGAACCUAGCCGCAAUC*stop*

5′D13
UCUCAAA----------CCGCACAGCCCCAAAUUUUACAAAACAGAAUAGAAUAAGAAUGAAAGUAAGAAUAGAAGCAAAGCAAU
GCAGAAGAAAAACAGCAGUAGAGAUGUGUUGGCAGUGAACCUAGCCGCAAUC*stop*